Verification of stable operation of rapid single flux quantum devices with selective dissipation

J. Hassel, L. Grönberg, and P. Helistö
VTT, P.O. Box 1000, 02044 VTT, Finland

It has been suggested that Rapid Single Flux Quantum (RSFQ) devices could be used as the classical interface of superconducting qubit systems. One problem is that the interface acts as a dissipative environment for a qubit. Recently ways to modify the RSFQ damping to reduce the dissipation have been introduced. One of the solutions is to damp the Josephson junctions by a frequency-dependent linear circuit instead of the plain resistor. The approach has previously been experimentally tested with a simple SFQ comparator. In this paper we perform experiments with a full RSFQ circuit, and thus conclude that in terms of stable operation the approach is applicable for scalable RSFQ circuits. Realisation and optimisation issues are also discussed.

INTRODUCTION

There is an ongoing effort to integrate Rapid Single Flux Quantum (RSFQ) technology [1] as the classical interface of qubit systems [2, 3, 4]. Despite the potential compatibility of the fabrication technology and the operating environment, it has been found that certain issues need to be resolved before functional RSFQ/Qubit systems are feasible. The basic question is to develop devices with sufficient functionality, which also preserve quantum coherence. The generic issues that have been addressed from the RSFQ side include fabrication [5, 6] and design [7, 8] solutions to decrease self-heating [9] as well as the control of the level of dissipation. The latter is important since the classical interface acts as a dissipative environment for a qubit. The level of dissipation experienced by the qubit can be reduced by choosing a low enough level of coupling between the RSFQ circuit and the qubits. This may degrade the functionality by limiting the signal levels seen by the qubit or by degrading the readout resolution. There are realisations of particular RSFQ components, which by design are less dissipative than the conventional ones [3, 4, 10]. Furthermore, unconventional damping schemes have been proposed which enable the design of generic RSFQ circuits with reduced dissipation. One such scheme is based on nonlinear shunts [11]. Another scheme is based on linear frequency dependent shunts, for which the damping resistor has been high-pass filtered by an appropriate circuit [12]. In the simplest form the filtering circuit consists of a capacitor C_s in series with the shunt resistor R_s. The $R_s C_s$ cutoff is to be chosen sufficiently below the plasma frequency ω_p of the Josephson junction (JJ). The principle of RC damping is illustrated in Fig. 1 together with a microscope photograph of a realisation using a Nb trilayer process [6].

To our knowledge, the experimental verification of the unconventional damping schemes is up to date limited to single JJs [11, 13] or SFQ comparators [12], though the
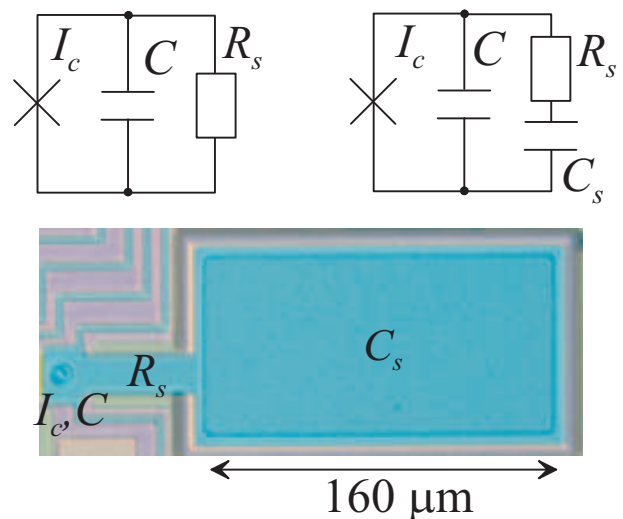

FIG. 1: Schematics of (a) The conventional and (b) RC damped Josephson junction. (c) A microscope photograph of an RC shunted Josephson junction realised by a Nb trilayer process.

functionality of complete RSFQ circuits has been verified by network simulations [12, 14]. In this paper we verify experimentally that complete RC shunted RSFQ devices function in a stable manner.

THE DEVICE

The circuit diagram and a microscope photograph of the device under study are shown in Fig. 2. The device is a Toggle flip-flop (TFF) driven by a DC/SFQ converter through a short section of Josephson Transmission Line (JTL). Apart from the damping arrangement the design of the circuit elements has been adopted from [1] and [15]. The dynamical sequence of the device is described as follows. As the input current I_{in} of the DC/SFQ converter is ramped up, at a certain treshold value the phase
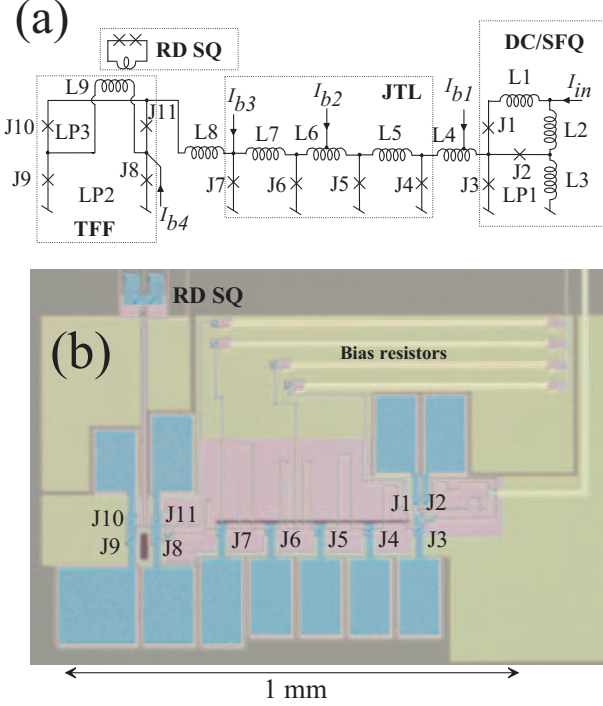
FIG. 2: The device used for verifying the stable operation of RC shunted RSFQ. (a) The equivalent circuit. The shunting circuits are not shown. The critical currents of junctions JN are $I_{c1}...I_{c6} = I_{c0}$, $I_{c7} = 1.06I_{c0}$, $I_{c8} = 1.12I_{c0}$, $I_{c9} = 1.42I_{c0}$, $I_{c10} = 0.89I_{c0}$ and $I_{c11} = I_{c0}$. Here $I_{c0} \approx 12$ μA. The JJ capacitances are $C_n \approx 0.3$ pF/μA$\times I_{cn}$. The shunt resistances and capacitances are chosen so that $\beta_c \approx 0.4$ and $\gamma \approx 0.1$. Inductances are $L_1 = 0.35L_0$, $L_2 = 0.33L_0$, $L_3 = 0.6L_0$, $L_4 = 0.4L_0$, $L_5 = 0.6L_0$, $L_6 = L_0$, $L_7 = 0.65L_0$, $L_8 = 0.35L_0$, and $L_9 = 1.33L_0$. Here $L_0 \approx 94$ pH. The bias current ratios are determined by on-chip bias resistors as $I_{b2}/I_{b1} = 0.95$, $I_{b3}/I_{b1} = 0.77$, $I_{b4}/I_{b1} = 0.77$. (b) A microscope photograph of the device.

of junction J3 rotates by 2π (J1 flips), which causes a flux quantum to propagate through the JTL to the TFF. The side-effect is that a persistent current flowing in loop LP1 changes causing junctions J1 and J2 to flip instead of J3 during the ramp-down. The ramp-down thus restores the original persistent current configuration in LP1, but has no other effect completing the DC/SFQ cycle. As a flux quantum enters the TFF either junctions in pair J8 and J10, or pair J9 and J11 flip depending on the value of the persistent currents in the TFF (loops LP2 and LP3). These events also change the value of the persistent current in LP2 and LP3 in such a way that subsequent events alternate the persistent current between two values corresponding to zero and one flux quanta through the loops. The above description thus confirms that the device utilises all the basic elements of RSFQ dynamics, namely the selection process as well as the propagation and the storage of flux quanta. The resulting simulated time-trace of the flux in LP2 is shown in Fig. 3(a).

The loop of the DC/SFQ converter is coupled to the loop of a readout dc SQUID (RD SQ) by a weak inductive coupling used to sense the state of the TFF. By replacing the RD SQ by a flux qubit, this type of an arrangement could be utilised for qubit manipulation. Here we are using the TFF - RD SQ arrangement as a SFQ/DC converter to be able to verify the proper operation of the circuit.

The device is fabricated by a Nb trilayer process, the VTT RSFQubit process [6] which fixes the critical current density $J_c = 30$ A/cm^2 for the JJs. The junction size is set to about 7 μm varying slightly depending on the design of the elements (see caption of Fig. 2 for details). All the junctions in the RSFQ circuit are damped with RC shunts. The hysteresis parameter for the JJs is $\beta_c = 2\pi I_c R_s^2 C/\Phi_0 \approx 0.4$, and the ratio of $R_s C_s$ cutoff and the JJ plasma frequency to about $\gamma = 1/R_s C_s \omega_p \approx 0.1$ [12]. This leads to typical physical values for the JJ and the shunt parameters values $I_c \approx 12$ μA, $C \approx 1.9$ pA, $R \approx 2.4$ Ω and $C_s \approx 35$ pF. The inductance values are of the order of 100 pH.

THE EXPERIMENT

The experiments were performed at liquid He by a conventional cryoprobe. The SFQ input signal and the bias currents (the SFQ bias and the RD SQ current and flux bias) were low-pass filtered by room temperature RC filters, and fed to the 4.2 K stage through twisted pairs of constantan wire. The RD SQ voltage output was amplified by a commercial room temperature preamplifier. An experimental plot is shown in Fig. 3(b). The similarity in comparison with the simulated data of Fig. 3(a) confirms that the device works in the desired mode described above. The difference in the time scales is irrelevant, since between the SFQ events the device is in the quiescent state. The shorter time scale is chosen in the simulation to minimise the computational effort. The only requirement is that the frequency of the DC/SFQ input signal I_{in} is much smaller than the inverse of the time scales of the SFQ events (here of order 100 ps). The only discrepancy between the simulation and the experiment is that the treshold current is slightly smaller (about 30 μA) in the experiment as compared to the simulation (about 50 μA). This may be partially explained by the difference in the designed and realised inductance values, but more likely the cause is partial flux trapping. The treshold current for a given device varied somewhat between different cooldowns, which supports this hypothesis. The treshold variation was also reproduced in simulations by applying flux to the loops of the DC/SFQ converter. The noise at the output voltage V_{RD} is well explained by the preamplifier voltage noise.
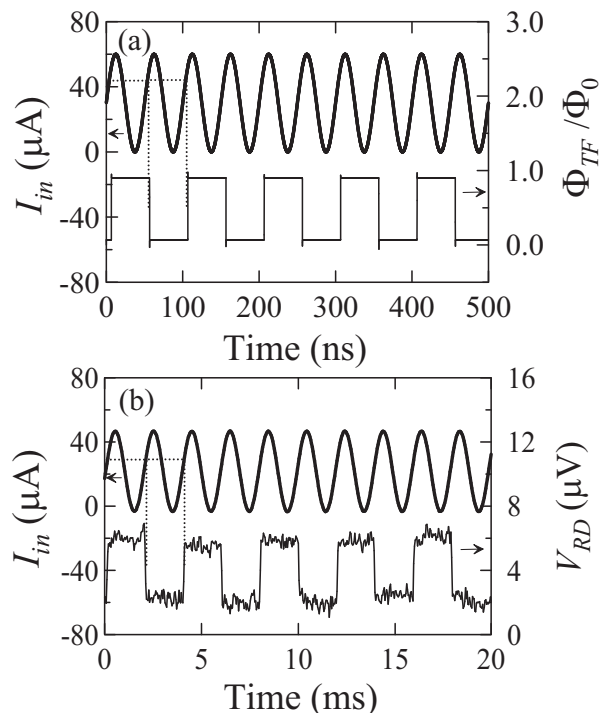
FIG. 3: (a) Simulated and (b) measured characteristics of the device. The thick line (left axis) is the input current of the DC/SFQ converter I_{in}. The thin line is the flux Φ_{TF} through loop LP2 of the TFF in (a) and the output voltage V_{RD} of the readout SQUID in (b) which is proportional to Φ_{TF}. The bias point is here $I_{b1} \approx 7\ \mu A$

DISCUSSION

Since our main aim is to verify here that the high-frequency damping alone suffices to stablise the devices, we briefly discuss the excess damping mechanisms present in our system. The current bias of the device is based on on-chip bias resistors of $R_b \gtrsim 40\ \Omega$ performing the required voltage-to-current conversion. The voltage is fed over an off-chip resistor (0.5 Ω) located near the chip at 4 K. Thus the bias resistor and the off-chip resistor form a loop of about 40 Ω in series with a bonding wire inductance of order 1 nH, i.e. the excess damping ranges roughly from DC to 5-10 GHz. As the worst-case the hysteresis parameter from bias resistors corresponds to $\beta_c \sim 100$, which is not enough to stabilise the system. The RD SQ, which is R-shunted, potentially causes some excess dissipation as well, which couples, however, to the RSFQ circuit only at high-frequencies ($\gtrsim 10$ GHz in our circuit). To ensure that the excess dissipation mechanisms do not stabilise our system, we removed the RC shunts and added the damping from the RD SQ and the bias resistors in the simulation. The result was that no stable operating point was found. It thus proved that the stabilisation of our system is in practise completely due to the RC shunts.

One issue in RC damped circuits is the parasitic resonance of the shunt capacitor. A sufficient criterion for avoiding this is that the capacitor dimension should be at maximum $\lambda_p/8$, where λ_p is the wavelength in the capacitor dielectric at the plasma frequency. This is given as $\lambda_p = 2\pi c/\omega_p \sqrt{\varepsilon_r (1 + 2\lambda_L/d)}$, where c is the speed of light, ε_r is the dielectric constant, λ_L is the London penetration depth of the electrodes, and d is the insulator thickness. In our case $\omega_p/2\pi = \sqrt{(1/2\pi\Phi_0)(I_c/C)} \approx 22$ GHz, $\varepsilon_r \approx 45$ (Nb$_2$O$_5$ dielectric), $\lambda_L \approx 85$ nm (Nb electrodes) and $d \approx 140$ nm. It follows in our case that $\lambda_p/8 \approx 170$ μm, which is also the maximum dimension we have used in the capacitors. However, in our geometry the lowest frequency resonance that could be excited is a $\lambda/2$ resonance corresponding to the long edge of the capacitor, so elements somewhat larger than this could be safely realised. In more general terms, parasitic resonances limit the maximum value of realizable capacitance. Since capacitance of a square with side w is $C_s = \varepsilon_r\varepsilon_0 w^2/d$, it follows $C_s \lesssim (\pi c)^2 \varepsilon_0/16\omega_p^2 d (1 + 2\lambda_L/d)$ from the requirement $w \lesssim \lambda_p/8$. In other words, realizability requires that

$$\gamma \gtrsim \frac{16\omega_p d (1 + 2\lambda_L/d)}{\pi^2 R_s c^2 \varepsilon_0} = \frac{32\sqrt{2}d (1 + 2\lambda_L/d)}{\pi \Phi_0 \varepsilon_0 c^2} I_c, \quad (1)$$

where we have used the definition of γ. In the last form we have also used the definitions of ω_p and β_c, and furthermore set $\beta_c = 1/2$, which is a typical value. Realizability thus gives the minimum γ.

From Eq. (1) we see that the minimum γ depends only λ_L, d and I_c. The maximum is determined from the stability requirement, which typically leads to $\gamma \lesssim 0.3$ [12]. The thickness d can be varied to some extent within fabrication tolerances. The dependence on I_c is, however, more important in terms of the optimisation of the RSFQ/qubit systems. The realizability and stability together set an upper limit for I_c. Low I_c is favorable also in terms of minimal self-heating of RSFQ components [7, 8, 9]. On the other hand, it was previously analysed that in case of a qubit inductively coupled to an RSFQ circuit, the minimisation of the dissipation favors an RSFQ circuit with large J_c [12]. Therefore it appears that at least in this coupling scheme the optimum solution would be a large-J_c process with small area junctions, e.g. sub-μm Nb junctions [16]. However, there may be other ways around this as well. It may be possible to relax the realizability restrictions by different implementations of the damping circuit. It also depends very much on the particular design whether the self-heating is a problem. For example, the device measured in this paper spends most of its time in the quiescent state, whence it should not heat very much above the bath temperature.

CONCLUSION

In conclusion we have successfully verified the stability of a RSFQ device based on selective damping realised by RC shunts. The device under study utilises all aspects of RSFQ dynamics. Our measurement scheme also gives direct evidence on SFQ events instead of the earlier measurement based on the statistical properties of a balanced comparator [12]. We therefore conclude that it is now experimentally verified that generic RSFQ devices can be realised by this damping scheme.

ACKNOWLEDGMENT

———————

[1] K. K. Likharev, and V. K. Semenov, IEEE Trans. Appl. Supercond. 1, 3 (1991).

[2] V. K. Semenov, and D. V. Averin, IEEE Trans. Appl. Supercond. 13, 960 (2003).

[3] D. V. Averin, K. Rabenstein, and V. K. Semenov, Phys. Rev. B 73, 094504 (2006).

[4] A. Fedorov, A. Shnirman, G. Schön, and A. Kidiyarova-Shevchenko, cond-mat/0611680 (2006).

[5] M. G. Castellano, L. Grönberg, P. Carelli, F. Chiarello, R. Leoni, S. Poletto, G. Torrioli, J. Hassel, and P. Helistö, Supercond. Sci. Technol. 19, 860 (2006).

[6] L. Grönberg, J. Hassel, P. Helistö, and M. Ylilammi, IEEE Trans. Appl. Supercond., in print.

[7] A. M. Savin, J. P. Pekola, D. V. Averin, and V. K. Semenov, J. Appl. Phys. 99, 084501 (2006).

[8] S. Intiso, J. Pekola, A. Savin, Y. Devyatov, A. Kidiyarova-Shevchenko, Supercond. Sci. Technol. 19, S335 (2006).

[9] A. M. Savin, J. P. Pekola, T. Holmqvist, J. Hassel, L. Grönberg, P. Helistö, and A. Kidiyarova-Shevchenko, Appl. Phys. Lett. 99, 084501 (2006).

[10] M. Wulf, X. Zhou, J. L. Habib, P. Rott, M. F. Bocko, and M. J. Feldman, IEEE Trans. Appl. Supercond. 13, 974 (2003).

[11] A. B. Zorin, M. I. Khabipov, D. V. Balashov, R. Dolata, F.-I. Buchholz, and J. Niemeyer, Appl. Phys. Lett. 86, 032501 (2005).

[12] J. Hassel, P. Helistö, H. Seppä, J. Kunert, L. Fritzsch, and H.-G. Meyer, Appl. Phys. Lett. 89, 182514 (2006).

[13] S. V. Lothkov, E. M. Tolkacheva, D. V. Balashov, M. I. Khabipov, F.-I. Buchholz, and A. B. Zorin, Appl. Phys. Lett. 89, 132115 (2006).

[14] A. B. Zorin, E. M. Tolkacheva, M. I. Khabipov, F.-I. Buchholz, and J. Niemeyer, Phys. Rev. B 74, 014508 (2006).

[15] S. V. Polonsky, V. K. Semenov, P. I. Bunyk, A. F. Kirichenko, A. Yu. Kidiyarova-Shevchenko, O. A. Mukhanov, P. N. Shevchenko, D. F. Schneider, D. Yu. Zinoviev, and K. K. Likharev, IEEE Trans. Appl. Supercond. 3, 2566 (1993).

[16] V. Patel, W. Chen, S. Pottorf, and J. E. Lukens, IEEE Trans. Appl. Supercond. 15, 117 (2005).